

DAMAGE INSPECTION METHOD OF RC RIGID FRAME VIADUCT USING NATURAL FREQUENCY AND MODE SHAPE

Fumiaki UEHAN¹ and Kimiro MEGURO²

ABSTRACT: This paper discusses a quick inspection method for earthquake-damaged railway viaducts. A new technique to inspect the damage levels of the upper and lower ends of a RC column is developed. Based on numerical simulations, damage judgment criteria to reflect the changes of the fundamental natural frequency and mode shape of a viaduct are presented. The vibration characteristics of damaged viaducts are investigated with microtremor measurements. The damage levels of the upper and lower ends of a column are judged by comparing the measured values with the proposed criteria.

Key Words: damage inspection, microtremor, model experiment, viaduct, AEM

INTRODUCTION

After the 1995 Kobe earthquake, a great number of RC columns were reinforced by steel jacketing (RTRI 1999). Due to the shear strengthening effect of the steel jacketing, it is expected that the flexural failure type mode will prevail in these viaducts (RTRI 1999). A RC column exhibiting flexural failure mode due to earthquake presents damage concentration at the upper and lower ends. If the damage level of the RC column ends is diagnosed, post-earthquake restoration works such as the selection of urgent remedies and/or the detection of defective retrofit construction are efficiently executed. Therefore, a new damage inspection method by using vibration measurements and judgment criteria developed by nonlinear numerical simulation is needed.

The authors have been developing a quick inspection method for earthquake damaged RC structures (Uehan and Meguro 2000a, 2000b). In this method, the structure natural frequency obtained by vibration measurements is used as the index of damage judgment. The damage judgment criteria are defined using the newly developed nonlinear simulation method named Applied Element Method (Meguro and Tagel-Din 1997). As the next step, a new method to inspect the damage levels of the upper and lower ends of a viaduct RC column is developed and discussed in this paper.

The main targets of the new inspection method are the RC viaducts of the Shinkansen. Since the Shinkansen viaduct is standardized, there are not so many types of superstructure and therefore it is not difficult to propose damage judgment criteria for each type of them. However, the cases to consider increase greatly if the combination of superstructure, foundation and soil is taken into account. In order to consider this, an efficient inspection technique for considering the influence of soil and foundation is proposed.

In the field of health monitoring of railway structures, inspection techniques use the vibrations induced by sources such as the moving train, impact on the structure (Nishimura and Tanamura 1998) and microtremors (Nakamura 1996). In this study, microtremor measurements are used in order to get the dynamic characteristics of the structure. The use of microtremor measurements is one of the most

¹ Researcher (Railway Technical Research Institute)

² Associate professor

Parametric study in order to obtain judgment indices

The damage judgment indices are obtained by the parametric study on the dynamic characteristics of the viaduct in various damage states. In this section, the soil and foundation are not taken into consideration and the superstructure of the viaduct is assumed to stand on a rigid foundation.

The ratios of natural frequency R_F and mode amplitude R_A that are defined by the next equations are used as the damage judgment indices.

$$R_F = F^d / F \quad (1)$$

$$R_A = A^{Top} / A^{Mid} \quad (2)$$

in which F^d : 1st mode natural frequency of damaged viaduct, F : 1st mode natural frequency of non-damage viaduct, A^{Top} : 1st mode amplitude at the top of column, A^{Mid} : 1st mode amplitude at the center of column (**Figure 3(a)**). The ratio of natural frequencies R_F is an index related to the damage level of the total viaduct system. The ratio of mode amplitudes R_A is an index related to the ratio of the damage level of the upper and lower ends of the column. The R_A is equal to 2.0 when the damage levels of the column upper and lower ends are equal. When the upper end is more damaged than the lower end, the R_A is larger than 2.0.

Procedure of vibration measurement

A preliminary measurement is performed in order to get F_G which is the 1st mode natural frequency of the non-damage viaduct with soil and foundation. If F_G is lower than F it means that the viaduct superstructure has no damage and the discrepancy is only due to the influence of the soil and foundation. The F of the Shinkansen viaduct is easily obtained through structural analysis. A post earthquake measurement is conducted in order to check the change of dynamic characteristics of viaduct. In this occasion, microtremors are measured at the top, middle and bottom of the column (**Figure 3(b)**). From the peak value of the Fourier spectra of microtremor records at the top, middle and bottom of the column, the 1st mode amplitudes, A_G^{Top} , A_G^{Mid} and A_G^{Bot} , are obtained. The predominant frequency of the viaduct after the earthquake is F_G^d .

Calculation of damage judgment indices

Assuming that the influence of the rotational component of soil-foundation spring can be disregarded, the damage judgment indices are obtained as follows. The ratio of mode amplitude R_A is calculated with the following equation.

$$R_A = A^{Top} / A^{Mid} \approx (A_G^{Top} - A_G^{Bot}) / (A_G^{Mid} - A_G^{Bot}) \quad (3)$$

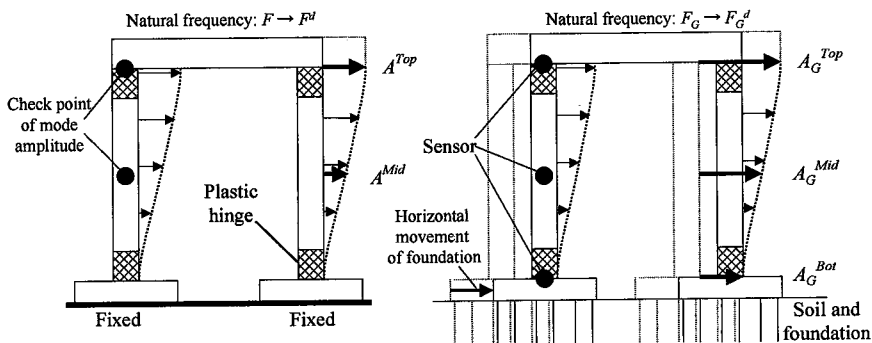


Figure 3. Deformation of damaged viaduct

The viaduct with soil and foundation is modeled as shown in **Figure 4**. The model is composed of the mass M , the horizontal spring K and the horizontal soil-foundation spring K_G . The natural frequencies F of the superstructure of the non-damaged viaduct and F_G of the non-damage viaduct with soil and foundation are calculated as follows.

$$F = \frac{1}{2\pi} \sqrt{\frac{K}{M}} \quad (4)$$

$$F_G = \frac{1}{2\pi} \sqrt{\frac{K \cdot K_G}{(K + K_G) \cdot M}} \quad (5)$$

When the viaduct stiffness decreases from K to K^d due to the column damage, these natural frequencies change to F^d and F_G^d , respectively, according to the following equations.

$$F^d = \frac{1}{2\pi} \sqrt{\frac{K^d}{M}} \quad (6)$$

$$F_G^d = \frac{1}{2\pi} \sqrt{\frac{K^d \cdot K_G}{(K^d + K_G) \cdot M}} \quad (7)$$

The ratio of natural frequencies R_F is obtained inserting equation (4) in (7).

$$R_F = F^d / F = F_G \cdot F_G^d / \sqrt{F^2 \cdot F_G^2 - F_G^{d2} \cdot (F^2 - F_G^2)} \quad (8)$$

Detection of stiffness reduction of soil-foundation spring

In the previous section, the foundation damage was not considered. Because the superstructure of the rigid frame viaduct is slender, there have been very few examples of damage to railway viaduct foundations. If soil liquefaction and/or soft ground lateral flow occur, most of the damage will concentrate on the viaduct foundation. In case that the stiffness of the viaduct decreases from K_G to K_G^{df} due to foundation damage, the ratio of stiffness of soil-foundation spring K_G^{df}/K_G is calculated as:

$$K_G^{df} / K_G = F_G^{d2} \cdot (F^2 - F_G^2) / F_G^2 \cdot (F^2 - F_G^{d2}) \quad (9)$$

Explanation and verification of proposed method by numerical simulation

Numerical model of railway viaduct with soil and foundation

By using the results of some numerical simulations, the proposed method is explained again and its validity checked. **Figure 5** shows the profile of the numerical model of railway RC viaduct with soil and pile foundation. The concrete and reinforcement steel Young's modulus are 28.0GPa and 200GPa, respectively. The girder is a 160ton rigid body. According to the numerical simulation, the natural frequency F of viaduct superstructure was 4.0Hz. The viaduct natural frequency F_G considering soil and pile foundation was 3.3Hz.

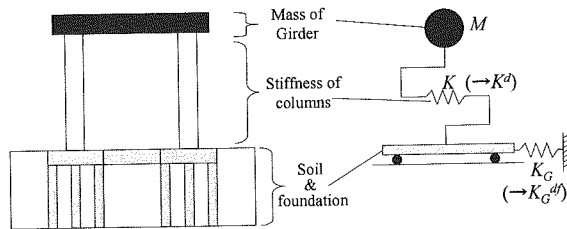


Figure 4. Simplified model of viaduct on the ground

Numerical simulation on nonlinear characteristic of Plastic hinge

Figure 6 shows the numerical model of an axially loaded RC column, the results of a cyclic loading simulation and the change of the 1st mode natural frequency of the RC column. The material properties and the axial load of the column model are the same as those of the viaduct model. Based on the simulation results, the stiffness of plastic hinge corresponding to each damage level (D1-D4) is obtained.

Parametric study for obtaining judgment indices

Figure 7 shows the simplified model of the viaduct superstructure. The stiffness of the plastic hinge corresponding to damage levels from D1 to D4 are substituted for the upper and lower ends of the model. Then, the damage judgment indices were calculated as shown in Table 1.

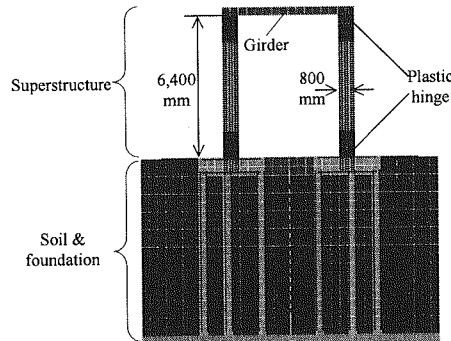


Figure 5. Numerical model of viaduct on the ground (using AEM)

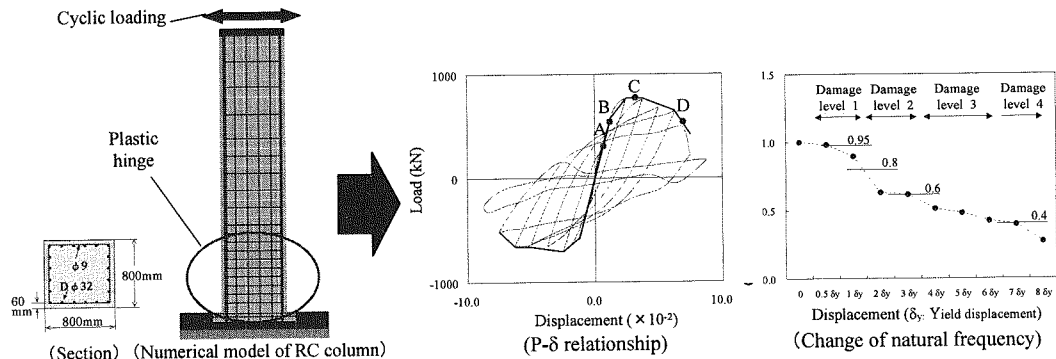


Figure 6. Numerical simulation on nonlinear characteristic of plastic hinge

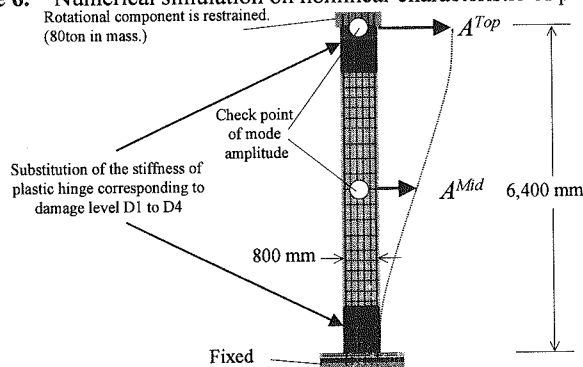


Figure 7. Simplified numerical model of viaduct (for AEM)

Table 1. Change of damage judgment indices due to damage to column ends

			Damage level of upper ends of column			
			D1	D2	D3	D4
Damage level of lower ends of column	D1	$R_F (=F^d/F)$	0.91	0.75	0.59	0.37
		$R_A (=A^{top}/A^{Mid})$	2.0	2.4	3.5	8.8
	D2	R_F	0.75	0.62	0.51	0.35
		R_A	1.8	2.0	2.7	5.8
	D3	R_F	0.58	0.51	0.44	0.32
		R_A	1.4	1.6	2.0	3.7
	D4	R_F	0.36	0.34	0.32	0.26
		R_A	1.1	1.2	1.3	2.0

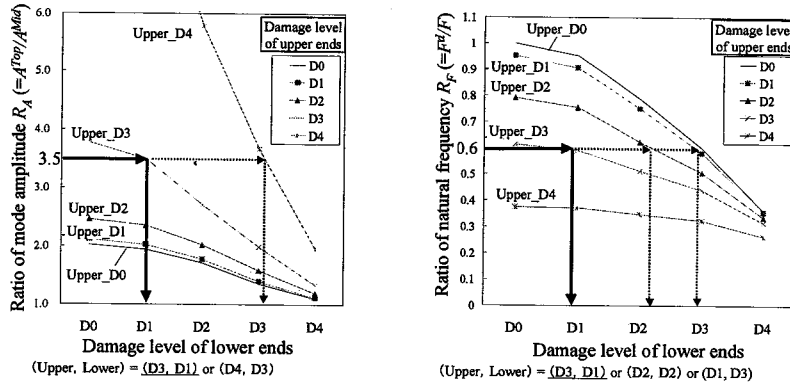


Figure 8. Judgment of damage condition of column ends

Calculation of judgment indices of numerical model and judgment of damage level

As an example, the judgment of a numerical model damage was carried out. First, the plastic hinges corresponding to D1 and D3 are substituted at the lower and the upper ends of the numerical model, respectively, as shown in **Figure 5**. According to the numerical simulation, the 1st mode natural frequency F_G^d was 2.2Hz, and the corresponding amplitudes A_G^{Top} , A_G^{Mid} and A_G^{Bot} were 1.0, 0.37 and 0.12, respectively. In this case, the damage judgment index $R_F (=F^d / F)$ is 0.60, and the $R_A (=A^{Top} / A^{Mid})$, 3.5. **Table 1** is summarized in **Figure 8** and the two indices are applied to the graphs. There was only one case (upper D3, lower D1) that meets the requirement of both indices, i.e. the damage level of the viaduct was correctly judged.

MICROTREMOR MEASUREMENTS ON EXPERIMENT MODEL

Microtremors were measured on a miniature rigid frame model in order to examine the accuracy of mode shape identification through microtremor measurements and to verify the efficiency of the proposed methods.

Outline on miniature model and measuring method

Figure 9 shows the profile of the frame model and the sensor arrangement. The steel model was fixed to the laboratory floor. The four columns support a girder load of 25kg. The joint stiffness was adjusted by using metal fittings and bolts. The used sensors were velocimeters of the type used for measurements on real structures. The sensors recorded simultaneously the horizontal component of the vibrations at the model top, center and bottom. The shelf for placing the central sensor was devised so that it would not affect the 1st mode natural frequency and mode shape of the model.

Identification of 1st mode shape of rigid frame model

The 1st mode shape of the rigid frame model is estimated under two conditions. In the first case, all joints are set rigid (**Figure 10(a)**). In the second case, the joints between column and girder are changed to the hinges (**Figure 10(b)**). In order to estimate the 1st mode shape of the frame model, the height of the sensor shelf is variously changed and the horizontal component of microtremors at girder, sensor shelf and at the base are simultaneously recorded every 0.01sec. The Fourier spectrum of the recorded data, 20.48sec, was smoothed using a Parzen spectral window. The peak value of the smoothed Fourier spectra obtained at girder, shelf and base are referred as A^{Girder} , A^{Shelf} and A^{Base} , respectively. The 1st mode amplitude A_h at the height of the sensor shelf is calculated with the following equation.

$$A_h = (A^{Shelf} - A^{Base}) / (A^{Girder} - A^{Base}) \quad (10)$$

The 1st mode shapes of the frame model estimated by microtremor measurement are shown in **Figure 11** together with the theoretical solutions. It is clear that the 1st mode shapes were well estimated with microtremor measurements.

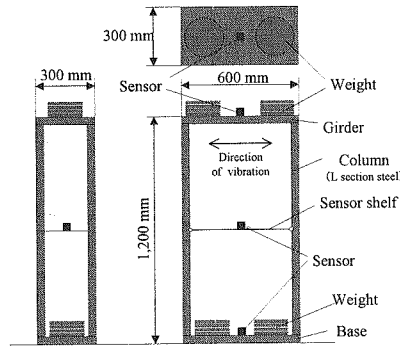


Figure 9. Outline of frame model and sensor arrangement

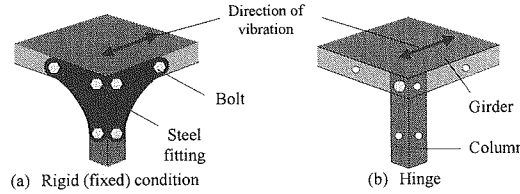


Figure 10. Conditions of frame model joints

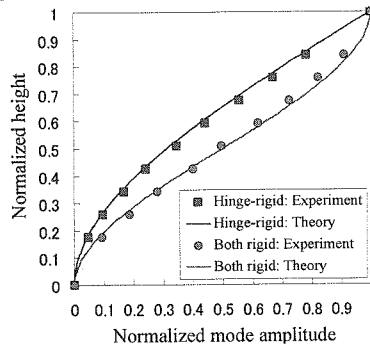


Figure 11. Mode shape estimated by microtremor measurement

Change of dynamic characteristics due to the damage to column

The change of dynamic characteristics due to damage to the frame model column ends is examined. The result estimated by microtremor measurements is compared with the results of numerical simulations. The three types of joint shown in **Figure 12** are used in order to change the joint stiffness of the frame model. The 1st mode natural frequency F^d and the ratio of mode amplitude $R_A (=A^{Top}/A^{Mid})$ of the frame model in each joints condition are examined. **Figure 13** and **Table 2** show the result of numerical simulation by the Applied Element Method. The stiffness and mass of each part of the numerical model shown in **Figure 12** are the same as those of the real frame model. **Table 3** shows the results of microtremor measurements. In this case, the height of the sensor shelf is 600mm (center of column) and the method of waveform processing is the same as the explained in the previous section. R_A is calculated by the reciprocal of equation (10). The analytical and experimental results agree well. These results indicate that the damage condition of column ends of structure can be detected by microtremor measurements.

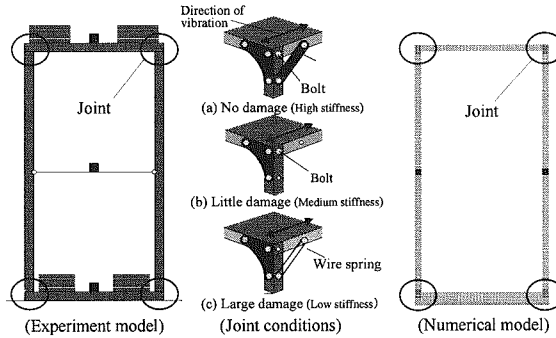


Figure 12. Outline of frame model and joint conditions

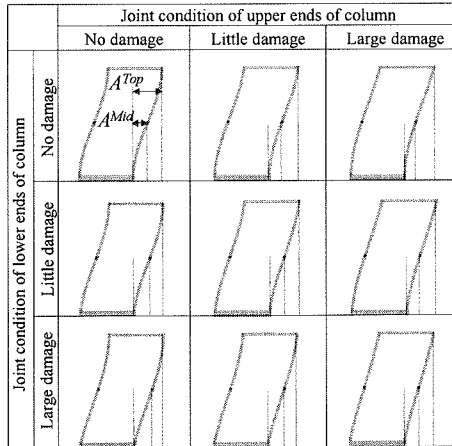


Figure 13. Mode shapes of damaged frame model by numerical simulation

Table 2. Change of dynamic characteristics due to damage to column ends (Numerical simulation)

			Type of joint between column and girder		
			(a)No damage	(b)Little damage	(c)Large damage
Type of joint between column and base	(a) No damage	F^d	4.2	3.7	3.0
		$R_A (=A^{Top}/A^{Mid})$	2.0	2.2	2.6
	(b) Little damage	F^d	3.7	3.3	2.7
		R_A	1.8	2.0	2.3
	(c) Large damage	F^d	3.0	2.7	2.2
		R_A	1.6	1.8	2.0

Table 3. Change of dynamic characteristics due to damage to column ends
(Experiment by using frame model without soil-foundation spring)

			Type of joint between column and girder		
			(a)No damage	(b)Little damage	(c)Large damage
Type of joint between column and base	(a) No damage	F^d	4.2	3.7	3.0
		$R_A (=A^{Top}/A^{Mid})$	2.0	2.2	2.5
	(b) Little damage	F^d	3.7	3.3	2.7
		R_A	1.8	2.1	2.3
	(c) Large damage	F^d	3.1	2.7	1.9
		R_A	1.6	1.8	2.0

Change of dynamic characteristics due to the damage to column ends (With soil-foundation spring)

Figure 14 shows the frame model with rubber bearing that imitated the soil-foundation spring. Microtremors were measured in this case following the same methodology presented in the preceding sections. The results of the measurement are shown in **Table 4**. F_G^d is the natural frequency of the frame model with rubber bearing whereas R_A is the ratio of mode amplitude ($=A^{Top}/A^{Mid}$). F^d was calculated by using equation (8) ($F=4.2\text{Hz}$). The F^d and R_A shown in **Table 4** correspond well to those of **Table 3**. These results indicate that the proposed method is effective even if the ground and foundation details are not clear.

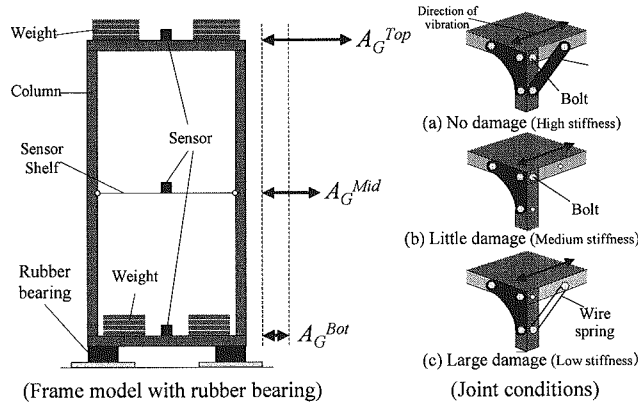


Figure 14. Outline of the frame model with soil-foundation springs

Table 4. Change of dynamic characteristics due to damage to column ends
(Experiment by using frame model with soil-foundation spring)

			Type of joint between column and girder		
			(a)No damage	(b)Little damage	(c)Large damage
Type of joint between column and base	(a) No damage	F_G^d	3.4	3.1	2.8
		F^d	4.2	3.7	3.2
		$R_A (=A^{Top}/A^{Mid})$	2.0	2.1	2.4
	(b) Little damage	F_G^d	3.1	2.9	2.5
		F^d	3.6	3.4	2.8
		R_A	1.8	1.9	2.2
	(c) Large damage	F_G^d	2.7	2.5	1.8
		F^d	3.0	2.7	1.9
		R_A	1.7	1.8	2.0

Detection of stiffness reduction of soil-foundation spring

Microtremors were measured for five combinations of frame and different soil-foundation springs. The natural frequency of the model (a), which does not have rubber bearing, is considered to be the natural frequency F of superstructure of non-damage viaduct. The natural frequency of the model (b) with normal rubber bearing is considered to be the natural frequency F_G of non-damage viaduct with soil and foundation. When the stiffness of the rubber bearing of the model (b) is K_G , those of model (c), (d) and (e) are $K_G/2$, $K_G/3$ and $K_G/4$, respectively. The natural frequency of models (c), (d) and (e) are considered the natural frequency F_G^{df} of viaduct with damaged foundation. **Table 5** shows the stiffness of rubber bearing, the natural frequency and the ratio of stiffness of soil-foundation spring K_G^{df}/K_G calculated by using equation (9). The change in the stiffness of rubber bearing was correctly detected.

Figure 5. Detection of stiffness reduction of soil-foundation spring

	(a)	(b)	(c)	(d)	(e)
Stiffness of rubber bearing	—	K_G	$K_G/2$	$K_G/3$	$K_G/4$
1st mode natural frequency F_G^{df} (Hz)	4.1(=F)	3.9(=F _G)	3.7	3.4	3.3
ratio of stiffness of soil-foundation spring K_G^{df}/K_G	—	1.0	0.52	0.33	0.25

CONCLUDING REMARKS

The authors proposed a damage inspection method of RC rigid frame viaduct. The method validity was checked by numerical simulations and model experiments. Dynamic characteristics such as the 1st mode natural frequency and mode shape of the frame model were accurately estimated by microtremor measurements. The change of dynamic characteristics due to the stiffness change of column ends or soil-foundation spring is also detected by microtremor measurement, and the proposed judgment indices indicated the value that the authors expected. Since the validity of the proposed method was confirmed in the model experiment, the future target is the verification of applicability of the proposed method to a real viaduct.

REFERENCES

- Meguro, K. and Tagel-Din, H. (1997) "A new efficient technique for fracture analysis of structures." *Bulletin of Earthquake Resistant Structure Research Center*, IIS, Univ. of Tokyo, No.30, 103-116.
- Nakamura, Y. (1996) "Real-time information systems for seismic hazards mitigation UREDAS, HERAS and PIC." *Quarterly Report of RTRI*, Vol. 37, No. 3, 112-127.
- Nishimura, A. and Tanamura, S. (1998). "A study on integrity assessment of railway bridge foundation." *RTRI Report*, Vol. 3, No. 8, 41-49, (in Japanese).
- RTRI. (1999). "Seismic design code for railway structures." Maruzen, Tokyo, Japan (in Japanese).
- Uehan, F. and Meguro, K. (2000a) "Improvement on quick inspection method for damaged RC structures using applied element method." *Bulletin of Earthquake Resistant Structure Research Center*, IIS, Univ. of Tokyo, No.33, 109-115.
- Uehan, F. and Meguro, K. (2000b) "Vulnerability assessment of jacketed viaduct using microtremor measurement & numerical simulation." *Proceedings of 12th World Conference of Earthquake Engineering (CD-ROM)*.